

Scalable Multi-robot Motion Planning for Congested Environments Using Topological Guidance

Courtney McBeth¹, James Motes¹, Diane Uwacu², Marco Morales¹, and Nancy M. Amato¹

Abstract—Multi-robot motion planning (MRMP) is the problem of finding collision-free paths for a set of robots in a continuous state space. The difficulty of MRMP increases with the number of robots due to the increased potential for collisions between robots. This problem is exacerbated in environments with narrow passages that robots must pass through, like warehouses. In single-robot settings, topology-guided motion planning methods have shown increased performance in these constricted environments. We adapt an existing topology-guided single-robot motion planning method to the multi-robot domain, introducing topological guidance for the composite space. We demonstrate our method’s ability to efficiently plan paths in complex environments with many narrow passages, scaling to robot teams of size up to five times larger than existing methods in this class of problems. By leveraging knowledge of the topology of the environment, we also find higher quality solutions than other methods.

I. INTRODUCTION

Multi-robot systems have become ubiquitous in many aspects of life. For example, in autonomous factories, industrial robots collaboratively assemble products and in warehouses, mobile robots navigate through shelves collecting orders. These applications feature many robots moving in proximity to each other within the environment. Highly coordinated multi-robot motion planning (MRMP) is required to avoid collisions with each other and with the environment

Existing MRMP approaches perform well in open environments but struggle with narrow passages (e.g. shelves in industrial warehouses or within department store aisles) due to the difficulty of avoiding collisions with obstacles within tight spaces. With multi-robot teams, narrow passages may be introduced or exacerbated by inter-robot collisions since robots must maneuver around each other within small spaces, further complicating planning. These inter-robot collisions can only be solved through coordination, limiting the effectiveness of decoupled approaches. Planning in the composite space (i.e. considering the joint planning space of all robots) provides this coordination; however, due to the large size of this space, it is computationally intractable.

Guided planning methods leverage external information to more efficiently find paths for single robots. These meth-

¹Courtney McBeth, James Motes, Marco Morales, and Nancy M. Amato are with the Parasol Lab, Department of Computer Science, University of Illinois Urbana-Champaign, Champaign, IL 61820 USA {cmcbeth2, jmotes2, moralesa, namato}@illinois.edu

²Diane Uwacu is with the Texas A&M University Department of Computer Science and Engineering, College Station, TX 77840 USA duwacu@tamu.edu

This work was supported in part by Foxconn Interconnect Technology (FIT) and the Center for Networked Intelligent Components and Environments (C-NICE) at UIUC.



Fig. 1. We demonstrate our method on a variety of physical and simulated environments. A video of these experiments can be found at <https://youtu.be/7j7hftwWJ98>

ods [1], [2] exploit topological representations of the environment to direct motion planning through narrow passages. In this work, we extend topological guidance to multi-robot systems in order to efficiently search the composite space.

Here, we present *Composite Dynamic Region-biased Rapidly-exploring Random Trees* (CDR-RRT), a coupled MRMP approach that utilizes workspace guidance to efficiently plan in the presence of narrow passages. By leveraging knowledge of the workspace topology, we more intelligently search the composite space, leading to improved planning times while retaining probabilistic completeness. We demonstrate a significant improvement in scalability compared to other state-of-the-art methods, successfully finding paths for teams of size up to five times larger than existing methods in complex environments where inter-robot collisions are likely to occur. Our contributions include:

- The development of composite-space analogs of workspace skeletons and sampling regions.
- A scalable, probabilistically complete MRMP method that leverages topological guidance.
- A theoretical analysis of the properties of the method.
- An experimental validation in a variety of congested and open environments with scaling robot team sizes.

II. PRELIMINARIES AND RELATED WORK

In this section, we discuss relevant motion planning preliminaries and related work in both the multi-robot motion planning and guided motion planning domains.

A. Motion Planning Preliminaries

A robot’s *degrees of freedom* (DOFs) include its position and orientation in the *workspace*, the 2D or 3D space within which the robot physically exists, as well as other

TABLE I
OVERVIEW OF RELATED METHODS

Algorithm	Coordination	Scalable	Probabilistic Completeness	Narrow Passages
CBS-MP [11]	Hybrid	X	X	
MRdRRT [12]	Hybrid	X	X	
Composite RRT	Coupled		X	
Composite PRM [13]	Coupled		X	
Decoupled PRM [13]	Decoupled	X		
CDR-RRT (Ours)	Coupled	X	X	X

configurable values such as joint angles. A *configuration* is a set of values describing the robot’s DOFs. The *configuration space* (\mathcal{C}_{space}) is the set of all robot configurations [3]. The *free space* (\mathcal{C}_{free}) is the subset of \mathcal{C}_{space} that only contains configurations that are not in collision with obstacles. The *obstacle space* (\mathcal{C}_{obst}) contains all configurations that are in collision with obstacles. Given a start configuration, q_{start} , and a goal configuration, q_{goal} , the *motion planning problem* strives to find a path from q_{start} to q_{goal} through \mathcal{C}_{free} .

Searching the entire \mathcal{C}_{space} is intractable [4], [5], resulting in the emergence of sampling-based motion planning algorithms [6], [7]. These algorithms forego completeness guarantees in favor of faster planning and *probabilistic completeness*, meaning that the probability of finding a solution, if one exists, converges to 1 in the upper limit of planning time. Unfortunately, these randomized sampling techniques suffer in constrained environments [8].

The underlying sampling-based motion planning algorithm that forms the basis of our method is Rapidly-exploring Random Trees (RRT) [7]. This method aims to iteratively grow a tree from q_{start} to q_{goal} . During each iteration, a random configuration q_{rand} is chosen from the \mathcal{C}_{space} . We then find q_{near} , the configuration in the existing tree closest to q_{rand} . A configuration some maximum distance Δ away from q_{near} in the direction of q_{rand} is added to the tree. RRTs exhibit a Voronoi bias that results in the rapid exploration of the \mathcal{C}_{space} and makes RRTs an efficient way to handle single-query motion planning problems. RRT variants have been developed to improve performance in the presence of narrow passages. Obstacle-based RRT (OBRRT) [9] grows an RRT along the edges of obstacles. Additionally, Dynamic-Domain RRT [10] adaptively manipulates its Voronoi bias to more efficiently explore constrained environments. However, these methods were designed for single-robot scenarios.

B. Multi-robot Motion Planning

Multi-robot motion planning consists of finding collision-free paths for a set of robots between their respective start and goal configurations. The composite \mathcal{C}_{space} is the Cartesian product of all individual robot \mathcal{C}_{spaces} . A composite configuration consists of values for each robot’s DOFs. The composite free space is made up of all configurations such that no individual robot is in collision with an obstacle or another robot. The MRMP problem can be formulated as finding a continuous path through the composite free space.

There are three classes of MRMP approaches. Table I shows an overview of select algorithms in each class.

Composite methods such as Composite PRM [13] and Composite RRT adapt single-robot sampling-based methods to plan directly within the composite \mathcal{C}_{space} . Other composite methods such as MRdRRT [12] and its variants [14], [15], build individual robot roadmaps and then search an implicit composite roadmap. These methods maintain the theoretical guarantees of the single-robot methods they use (probabilistic completeness [12] and asymptotic optimality [14], [15]). However, due to the decoupled individual roadmap construction, they struggle in environments with narrow passages.

Decoupled approaches such as Decoupled PRM [13] plan individual robot paths in their own decoupled \mathcal{C}_{spaces} . These approaches are typically faster and allow for linear scaling with respect to the number of robots, but do not offer completeness or optimality guarantees. The lack of completeness degrades their performance in the presence of narrow passages, where inter-robot collisions are likely.

Hybrid methods such as CBS-MP [11], ECBS-CT [16], and M* [17] seek to leverage the strengths of both composite and decoupled methods. For example, CBS-MP [11] plans individual robot paths in their decoupled \mathcal{C}_{spaces} and then reconciles the paths in the composite \mathcal{C}_{space} . In the worst case, these methods will explore the whole composite \mathcal{C}_{space} , but on average, the runtimes are comparable to the decoupled methods while providing varying levels of (probabilistic) completeness and (representation) optimality guarantees. Like decoupled approaches, these methods are generally not well suited for environments with narrow passages.

C. Guided Motion Planning

Several single-robot motion planning strategies have been proposed to guide the planner through the workspace; however, this has not been well explored in the composite space. The Feature Sensitive Motion Planning Strategy [18] subdivides the environment into homogeneous workspace regions that are planned in individually, adapting roadmap construction to local features. The individual roadmaps are merged into a complete roadmap of the planning space. This strategy allows the planner to use resources efficiently.

Workspace Decomposition Strategies [19]–[21] help bias planning towards narrow areas of the workspace. SyClop [22] uses an RRT to sample frontier decomposition regions. A User-Guided Planning Strategy [23] allows the user to define and manipulate workspace sampling regions that the planner explores in real-time. The planner relies on the user’s intuition to explore narrow passages and find paths faster.

Skeleton-based strategies leverage the topology of the workspace, which is represented by a workspace skeleton (Fig. 2(a)), an embedded graph. Examples include medial axis skeletons [24] in 2D and mean curvature skeletons [25] in 3D. Skeleton edges describe contiguous volumes of the free workspace (e.g. tunnels or rooms). Skeleton vertices represent connections between these volumes. The skeleton is homotopy equivalent to the workspace. All points in the workspace can be smoothly collapsed to the skeleton [26].

Dynamic Region Sampling with PRM (DR-PRM) [2], initiates local components at the vertices of a topological

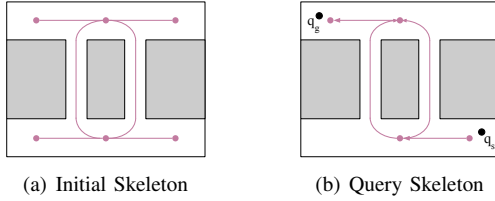


Fig. 2. An example workspace skeleton (a) and query skeleton (b). The query skeleton is a directed and pruned skeleton that only contains edges along a path from q_{start} to q_{goal} .

Algorithm 1 Dynamic Region-biased RRT

Input: Environment e and a Query $\{q_s, q_g\}$
Output: Tree T

- 1: $W \leftarrow \text{COMPUTESKELETON}(e)$
- 2: $S \leftarrow \text{COMPUTEQUERY SKELETON}(W, q_s, q_g)$
- 3: $T \leftarrow (\emptyset, \emptyset)$
- 4: $R \leftarrow \text{INITIALREGIONS}(S, q_s)$
- 5: **while** $\neg done$
- 6: $\text{REGIONBIASEDRRTGROWTH}(T, S, R)$
- 7: **return** T

skeleton, and expands them along adjacent edges, then merges them to form a complete roadmap. It is mostly applied to handle multi-query motion planning problems. We describe its single-query counterpart, Dynamic Region-biased RRT (DR-RRT), in greater detail in Section II-D since we extend our method from it. These methods show the advantage of leveraging workspace information to guide planning in C_{space} when they are closely related; however, they are constrained to single-robot settings, limiting their applicability to many multi-robot use cases including autonomous warehouse navigation.

D. Dynamic Region-biased RRT

DR-RRT [1] grows an RRT while constraining sampling to be within regions that advance along a workspace skeleton.

1) *Query Skeleton:* Algorithm 1 [1] creates two skeletons: one for the entire workspace (line 1), and the *query skeleton* (Fig. 2(b); line 2), which retains only edges that are along a path from the start to the goal in the workspace. Sampling regions will advance along the edges of the query skeleton.

2) *Sampling Regions:* The construction of the RRT begins by initializing the first region centered on the skeleton vertex closest to q_{start} (line 4). A *region* is any bounded volume of the workspace, e.g., a bounding sphere or an axis-aligned bounding box. During each iteration of DR-RRT (Alg. 2) [1], one existing region is selected to guide sampling (line 1). The probability of each region being chosen is proportional to its *extension success rate*. With a small probability ϵ , the entire environment will be chosen to sample from. A random configuration q_{rand} is selected from this region toward which to grow the tree (line 3). The algorithm then proceeds as a general RRT by attempting to extend the tree to q_{new} (line 4). The extension success rate is updated based on the success or failure of this attempt (lines 7-10).

Algorithm 2 Region-biased RRT Growth

Input: Tree T , Query Skeleton S , Regions R , region radius η , maximum for failed extension attempts τ

- 1: $r \leftarrow \text{SELECTREGION}(R)$
- 2: $q_{rand} \leftarrow r.\text{GETRANDOMCFG}()$
- 3: $q_{near} \leftarrow \text{NEARESTNEIGHBOR}(T, q_{rand})$
- 4: $q_{new} \leftarrow \text{EXTEND}(q_{near}, q_{rand}, \Delta)$
- 5: **if** $r = \emptyset$ \triangleright The entire environment was chosen
- 6: **return**
- 7: **if** $q_{new}.\text{EXTENSIONSUCCEEDED}()$
- 8: $r.\text{INCREMENTSUCCESSSES}()$
- 9: **else**
- 10: $r.\text{INCREMENTFAILURES}()$ \triangleright Choose new region
- 11: **for** $r \in R$
- 12: **while** $r.\text{INREGION}(q_{new})$
- 13: $r.\text{ADVANCEALONGSKELETONEDGE}()$
- 14: **if** $r.\text{ATENDOF SKELETONEDGE}()$
- 15: $R \leftarrow R \setminus \{r\}$
- 16: **if** $r.\text{NUMFAILURES}() > \tau$
- 17: $R \leftarrow R \setminus \{r\}$
- 18: **for all** $v \in S.\text{UNEXPLOREDVERTICES}()$
- 19: **if** $\delta(v, q_{new}) < \eta$
- 20: $R \leftarrow R \cup \text{NEWREGION}(v)$
- 21: $S.\text{MARKEXPLORED}(v)$

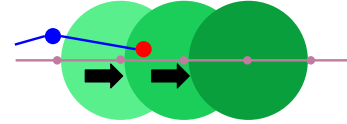


Fig. 3. An example of region advancement. The roadmap is shown in blue with q_{new} in red. The region advances, centered on intermediates along the skeleton edge, from its initial position in light green (leftmost) along the skeleton edge until it reaches the position shown in dark green (rightmost) where it is no longer in contact with q_{new} .

3) *Region Advancement:* Once a configuration has been added to the tree, all existing regions that are in contact with q_{new} are advanced forward along their skeleton edges until they leave q_{new} behind them (lines 11-13). This is illustrated in Fig. 3. If a region reaches the end of its edge, it is deleted (lines 14-15). Then, new regions are created on each unexplored query skeleton vertex that is within a small distance of q_{new} (lines 18-21). This cycle of region selection, tree extension, region advancement, and region creation continues until the tree extends to q_{goal} .

III. COMPOSITE DYNAMIC REGION-BIASED RRT

Here, we detail how we extend DR-RRT to multi-robot systems to propose a new method, Composite Dynamic Region-biased RRT (CDR-RRT). We do this by developing composite analogs for workspace skeletons and regions that allow for coupled multi-robot motion planning.

The composite space size is exponential in the number of robots. Thus, efficient planning requires limiting exploration of the composite space to areas that are likely to yield a

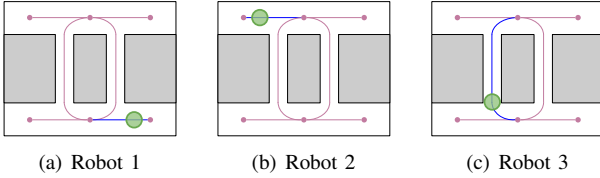


Fig. 4. An example of a composite edge and a composite region. Each of the three robots has its own workspace skeleton. Obstacles are gray, and the workspace skeletons are purple. Three skeleton edges that comprise a composite edge are shown in blue. All possible combinations of such edges make up the composite workspace skeleton. Three individual regions that make up a composite region along this composite edge are shown in green.

Algorithm 3 Grow Composite Workspace Skeleton

Input: Composite Workspace Skeleton S , Composite Regions R , Composite Source Vertex V , maximum number of edges to explore per vertex μ , maximum number of active regions ρ

- 1: $C \leftarrow \{\}$ $\triangleright C$ stores new vertices and their costs
- 2: **for all** $V' \in V.GETNEIGHBORS()$
- 3: $C \leftarrow C \cup \{(V', HEURISTICCOST(V'))\}$
- 4: **while** $C \neq \emptyset$ and $|V.OUTGOINGEDGES()| < \mu$
- 5: $U \leftarrow C.POPNEXTBESTVERTEX()$
- 6: $S.ADDVERTEX(U)$
- 7: $S.ADDEDGE(V, U)$
- 8: **if** $|R| < \rho$
- 9: $R \leftarrow R \cup \text{NEWREGION}(EDGE(V, U))$
- 10: **else**
- 11: $V.ADDUNEXPLOREDEGE(V)$

solution. We leverage lazy construction of the composite skeleton structure as we search the composite space. We also exploit a greedy heuristic to search along this constructed skeleton while finding a collision-free path for all robots.

A. Composite Skeleton

A composite skeleton (Fig. 4) is the Cartesian product of the workspace skeletons corresponding to each of the n robots. It consists of composite vertices and edges representing all combinations of vertices and edges in the n individual robots' workspace skeletons respectively. The size of the composite workspace skeleton is exponential in the number of robots. A composite region is made up of n individual sampling regions, one in each robot's workspace.

Computing a composite query skeleton, which is a directed and pruned version of the composite workspace skeleton, requires an explicit computation of the composite workspace skeleton. Instead, we heuristically prune the composite skeleton, retaining a maximum of μ lowest-cost outgoing composite edges for each explored composite vertex. These edges are likely to be along a feasible low-cost path from q_{start} to q_{goal} . The number of retained edges μ should be dependent on the likelihood of inter-robot collisions along direct paths for each robot. Retaining more edges allows more alternate paths to be explored to avoid inter-robot conflicts. We discuss a cost heuristic to capture this likelihood in Section III-C.

Algorithm 4 Composite Region-biased RRT Growth

Input: Tree T , Composite Skeleton S , Regions R , maximum for failed extension attempts τ

- 1: $r \leftarrow \text{SELECTCOMPOSITEREGION}(R)$
- 2: $q_{rand} \leftarrow r.GETRANDOMCOMPOSITECFG()$
- 3: $q_{near} \leftarrow \text{NEARESTNEIGHBOR}(T, q_{rand})$
- 4: $q_{new} \leftarrow \text{EXTEND}(q_{near}, q_{rand}, \Delta)$
- 5: **if** $r = \emptyset$ \triangleright The entire environment was chosen
- 6: **return**
- 7: **if** $q_{new}.EXTENSIONSSUCCEEDED()$
- 8: $r.INCREMENTSUCCESSSES()$
- 9: **else**
- 10: $r.INCREMENTFAILURES()$ \triangleright Choose new region
- 11: **for** $r' \in \text{SIBLINGREGIONS}(r)$
- 12: **while** $r'.INCOMPOSITEREGION(q_{new})$
- 13: $r'.ADVANCEALONGCOMPOSITESKELETONEDGE()$
- 14: **if** $r'.ATENDOFCOMPOSITESKELETONEDGE()$
- 15: $V_t \leftarrow r'.COMPOSITETARGETVERTEX()$
- 16: $S.GROWCOMPOSITESKELETON(V_t)$
- 17: $R \leftarrow R \setminus \{r'\}$
- 18: **if** $r.NUMFAILURES() > \tau$
- 19: $r.CREATENEXTBESTREGION()$
- 20: $R \leftarrow R \setminus \{r\}$

B. Guided Composite RRT Construction

To begin RRT construction, we compute the first composite skeleton vertex and each neighboring composite edge and vertex. Algorithm 3 shows how composite vertices and edges are created to grow the composite skeleton from a composite vertex. We start with composite vertex V_{start} that represents the set of $v_{start}^{(i)}$ for all robots $i \in \{1, \dots, n\}$, with $v_{start}^{(i)}$ being the individual workspace skeleton vertex closest to q_{start} for robot i . CDR-RRT then proceeds as DR-RRT by iteratively performing region selection, sampling, RRT growth, region advancement and deletion, and new region creation until q_{goal} is reached (Alg. 4).

1) *Sampling Regions:* The size of the explored composite skeleton becomes exponentially larger as new vertices are visited. To reduce memory usage and preserve a high probability of selecting low-cost regions, we limit the maximum number of active sampling regions at any time to ρ . The value of ρ determines the trade-off between exploration and exploitation. A larger ρ allows for multiple areas of the composite skeleton to be explored concurrently. A smaller ρ allows for the lowest-cost edges of the composite skeleton to be traversed more quickly. Because our cost heuristic is able to capture the potential for inter-robot conflicts well, it is generally sufficient to use as few as one active region to efficiently find a path. It is possible, however, that better paths may be found by exploring a larger portion of the composite skeleton using a larger set of active regions. We denote the set of active regions as R . Let c_r be the cost of region r and c_{max} be the maximum cost of any active region. Let s_r be the extension success rate of the region

r as in DR-RRT [1]. We establish a probability distribution over the active regions where the probability, p_r , of selecting region r is shown below.

$$p_r = \frac{s_r \cdot e^{(c_{max} - c_r)}}{\sum_{r' \in R} s_{r'} \cdot e^{(c_{max} - c_{r'})}}$$

Using an exponential function ensures that low-cost regions are much more likely to be sampled from. Multiplying by the extension success rate reduces the probability of selecting a region that often fails to extend.

2) *Region Advancement*: After sampling from composite region r and extending the tree, we advance all sibling composite regions of r forward until they leave q_{new} behind (lines 11-13). Sibling regions are those that lie upon edges with the same source vertex. An example of this process is shown in Fig. 5. In single-robot DR-RRT [1], all regions are advanced whenever a new configuration is added to the tree; however, due to the large size of the composite space, q_{new} is unlikely to lie within a region unless q_{rand} was sampled from a nearby region. By restricting advancement to sibling regions, we leverage spatial locality to reduce the amount of computation necessary to execute region advancement while maintaining performance.

In DR-RRT [1], as individual regions advance along skeleton edges, they are centered on intermediate points along those edges. Correspondingly, we create composite intermediates along composite skeleton edges. During composite region advancement, as can be seen in Fig. 5, all individual regions are advanced forward the minimum amount of intermediates such that the composite region is no longer touching q_{new} .

The composite edge intermediates are chosen at a granularity in the composite space such that there are an equal number of individual intermediates along each of the individual edges that make up the composite edge. These individual edge lengths may be different and, thus, the distances between the individual intermediates may vary for each robot. As a result, as a group traverses a composite edge, some robots may move faster than others. This could be prevented by splitting individual skeleton edges into pieces of roughly the same length; however, this approach comes at the expense of increasing the size of the composite skeleton. Due to the increase in running time incurred by this modification, we opted to leave the individual skeletons unchanged.

When a composite region reaches the target vertex of the edge it lies upon, it is deleted (lines 14-17), and the composite workspace skeleton is grown by adding a maximum of μ outgoing edges from this composite vertex (Alg. 3). Up to ρ new regions are spawned on these new composite edges. Unexplored edges are stored in a priority queue based on their cost. When a region surpasses τ failed extension attempts, it is deleted and replaced with a region on the lowest cost edge from the priority queue (lines 18-20).

C. Multi-agent Pathfinding Heuristic

We assign a cost to each composite skeleton edge using a multi-agent pathfinding heuristic and choose the cost of a

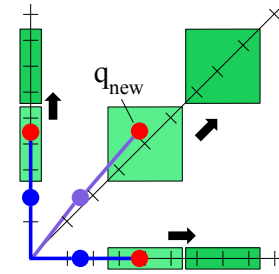


Fig. 5. An example of composite region advancement for two point robots in a 1D environment. The individual robots' skeletons are shown on the axes and the composite skeleton between them. Each individual roadmap is shown in blue and the composite roadmap is in purple. Edge intermediates are shown as tick marks along the skeletons. Both individual regions advance at the same rate with respect to their individual intermediates until the composite region leaves q_{new} behind at the position shown in dark green.

region to be equivalent to the cost of the composite skeleton edge it lies upon. Multi-agent pathfinding (MAPF) is the discrete state space equivalent of the multi-agent motion planning problem. As an implementation choice, we adapt Conflict-Based Search (CBS) [27] to the space. CBS uses a hierarchical approach with a low-level search to find individual paths for each agent and a high-level search to resolve conflicts between individual paths.

Let V_{goal} represent the composite skeleton vertex closest to q_{goal} and $v_{goal}^{(i)}$ represent the vertex closest to q_{goal} for robot i in its individual workspace skeleton. We define the cost of a composite skeleton edge in terms of the maximum individual path length from the composite edge's target vertex, V_t , to $v_{goal}^{(i)}$ for a robot on its individual skeleton. This value is a lower bound estimate of the number of composite skeleton edges needed to be explored to find a path from V_t to V_{goal} . We ensure that these individual paths are feasible by accounting for potential collisions between robots traversing their individual skeletons. We define the capacity of an individual skeleton edge as the minimum width between obstacles along the edge. If the total width of the robots traversing that edge exceeds the capacity, a conflict has occurred. These conflicts are resolved by CBS's high-level search. In the case where individual skeletons vary between robots, CBS variants such as CBS-MP [11] can be adapted to the space.

D. Memory Optimization

The size of the full composite skeleton is exponential in the number of robots, so we optimize memory usage by leveraging local, on-demand construction of the composite skeleton. We can also remove composite vertices and edges when they are no longer useful. A composite edge is no longer useful when the composite region that traverses it has reached the end and been deleted. A composite vertex is no longer useful when all of its incoming and outgoing edges are no longer useful.

IV. THEORETICAL ANALYSIS

During each iteration of CDR-RRT, there is a probability $\epsilon > 0$ of sampling from the entire environment rather

than within a region (Alg. 4). Sampling from the entire environment guarantees probabilistic completeness, ensuring that a valid path from q_{start} to q_{goal} will be found, if one exists, even if all regions are unable to produce valid configurations. As ϵ increases to 1 or as the size of regions is increased to encompass the entire workspace, knowledge of the workspace topology is utilized less and the method eventually reduces to Composite RRT.

V. VALIDATION

We run scaling MRMP queries in 2D and 3D environments designed to highlight the strengths and weaknesses of our approach. We consider robot teams of 2, 4, and 6, in addition to a single scaling experiment with up to 12 robots. We increase the environment size proportionally with the robots. We scale the narrow passage widths in select environments to measure the impact of the complexity of the environment on the performance of each approach.

We compare to several state-of-the-art MRMP methods (Table I). We use a CBS-MP [11] variant that uses DR-PRM [2] to construct the individual roadmaps (CBS-DR-PRM) as a comparison against a hybrid method with workspace guidance. Although MRdRRT [12] was designed primarily for manipulators, we feel it is necessary to compare against it because its use of a tensor-product roadmap to conduct an RRT-style search of the composite space is similar to our composite workspace skeleton guidance.

All methods were implemented in C++ in the Parasol Planning Library. All experiments were run using a desktop computer with an Intel Core i9-10900KF CPU at 3.7 GHz and 128 GB of RAM. Each method is given 600 seconds to find a plan or is considered unsuccessful.

A. Environments

In this section, we describe our experimental environments and explain why these scenarios highlight the advantages and disadvantages of our approach relative to other methods.

1) *Warehouse (Fig. 6)*: This scenario is designed to imitate the motions required to fetch or place items on shelves in a warehouse or department store. The topology creates several parallel narrow passages, and queries are selected such that conflicting choices of aisles are likely, thus requiring coordination during planning to avoid inter-robot collisions. In one version, the aisles can only be entered at the top or bottom (Fig. 6(a)-6(c)). The other version includes a width-wise aisle cutting through the middle of the length-wise aisles creating entry/exit points that can be used to avoid collisions (Fig 6(d)-6(f)). We scale the number of aisles with the number of robots. For each version, we consider three variants with progressively doubled aisle widths.

2) *Open Cross (Fig. 7(a))*: We evaluate our approach on a classic open MRMP scenario [11] to demonstrate how our method compares when workspace is not informative, limiting the benefit of topological skeleton guidance.

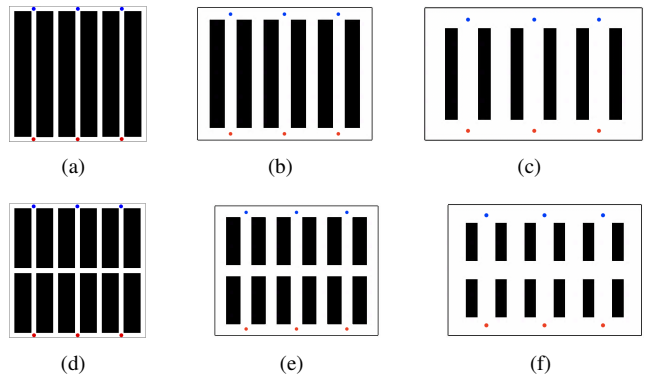


Fig. 6. The Long (a-c) and Short (d-f) Warehouse scenarios both have three variants with progressively wider aisles. The robots on top and bottom must swap places with the robot with which they are aligned vertically.

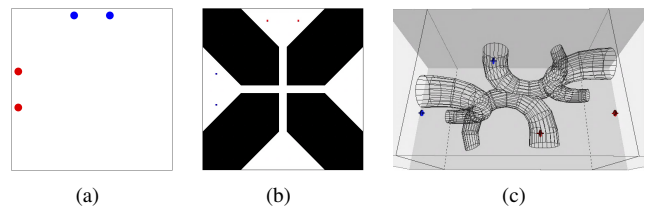


Fig. 7. In both the Open Cross (a) and Funnel Cross (b) environments, the red robots must move from left to right and the blue robots from top to bottom. In the Maze Cross (c) environment, robots starting on the left and right must swap places by moving through the 3D tunnel structure.

3) *Funnel Cross (Fig. 7(b))*: We modify the open cross MRMP scenario to create a pathological narrow passage problem. Both the robots moving top to bottom and left to right must pass through a funnel. These funnels intersect at the narrowest point resulting in an extremely narrow passage in the composite \mathcal{C}_{space} through which the path must pass.

4) *Maze Cross (Fig. 7(c))*: In this 3D environment with a narrow maze tunnel, the number of degrees of freedom of each mobile robot is doubled relative to a 2D workspace, resulting in a very large composite space.

5) *Inlet (Fig. 8)*: This small scenario requires high coordination to solve. We show how each method performs when one robot must explicitly move out of the other’s way.

B. Narrow Passages

The Warehouse scenarios demonstrate the performance of each method in with varying widths of narrow passages (results in Fig. 9). Decoupled PRM was unable to complete the 2-robot scenarios and is omitted from the plots. Composite RRT achieves the lowest planning time on all 2-robot scenarios and the widest 4-robot Long Warehouse variant but is unable to scale to more complex 4 and 6-robot scenarios. CDR-RRT’s use of composite skeleton guidance improves its performance relative to Composite RRT on these more complex 4 and 6-robot scenarios, where it performs the best.

C. Robot Crossings

The Open Cross, Funnel Cross, and Maze Cross environments evaluate each method’s performance in different robot

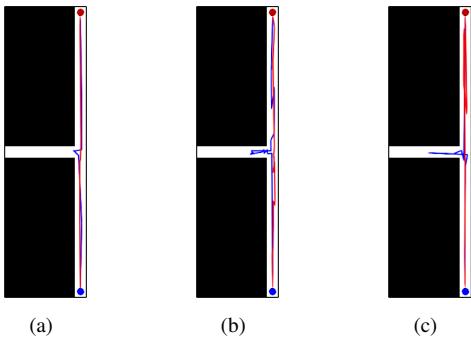


Fig. 8. In the Inlet environment, the red and blue robots must swap places. One robot must move out of the way to allow the other to pass. Example paths are shown for CDR-RRT (a), Composite RRT (b), and Composite-PRM (c). CDR-RRT find a smoother, lower cost path.

cross scenarios, in which topological guidance provides varying levels of benefit. The Open Cross environment results are in Fig. 10(a). When the topology is not useful, workspace guidance still biases robot paths along skeleton edges, which, in an environment without obstacles, increases the potential for collision relative to Composite RRT and Composite PRM. As a result, CDR-RRT has a higher average planning time than Composite RRT and Composite PRM. This shows that composite skeleton guidance is most effective when there are narrow passages that robots must pass through.

CDR-RRT achieves the fastest average planning time on each of the 2, 4, and 6-robot Funnel Cross scenarios (Fig. 10(b)). CDR-RRT’s efficient search of the composite space results in high performance in environments with extremely narrow passages with scalability to larger robot teams.

In the Maze Cross scenarios (10(c)), Decoupled PRM failed to solve the 2-robot scenario and is omitted. CBS-DR-PRM has a slightly lower average runtime for 2 robots but lacks the coordination required to solve the 4-robot scenario, which CDR-RRT is able to complete. In 3D environments, the size of the composite \mathcal{C}_{space} increases significantly, necessitating the use of composite skeleton guidance.

D. Coordination

The Inlet scenario results are given in Fig. 11. CBS-DR-PRM and MRdRRT were unable to find solutions within the time limit. The runtimes for CDR-RRT, Composite RRT, and Composite PRM were similar; however, the solution quality varies greatly between the three methods. Defining the cost metric as the longest individual path, CDR-RRT has an average path cost of 12.68 meters, while Composite RRT and Composite PRM have average path costs of 18.15 and 16.18 meters respectively. Example paths for these methods are shown in Fig. 8. By following the composite skeleton, CDR-RRT finds a more direct, lower-cost path. We also demonstrate our method on physical robots (Fig. 1).

E. Scalability

We ran 8, 10, and 12-robot Long Warehouse scenarios with a 3-hour time limit for CDR-RRT to measure its performance on larger problems. Fig. 12 shows that CDR-RRT is able to

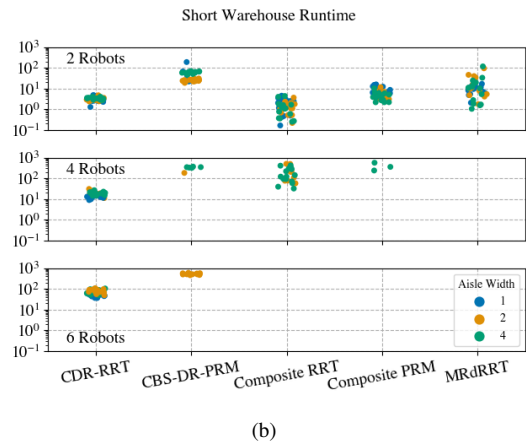
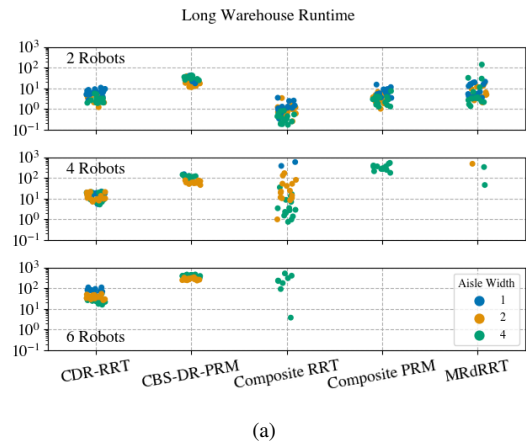


Fig. 9. Running time results for the Long (a) and Short (b) Warehouses.

efficiently find paths for the 8-robot and less complex 10-robot variants. However, its performance begins to degrade in the narrowest aisle variant of the 10-robot scenario due to the difficulty of resolving up to five inter-robot collisions simultaneously within a very small space. Only the least narrow 12-robot variant was able to be completed within the time limit, demonstrating the large impact of narrow passage width in resolving inter-robot collisions.

VI. CONCLUSION AND FUTURE WORK

We present Composite Dynamic Region-biased Rapidly-exploring Random Trees, a scalable workspace-guided multi-robot motion planning approach. We validate our method on a variety of environments, with and without narrow passages, to demonstrate its strengths and weaknesses. We show improved performance in constricted environments. Future work will explore the use of composite workspace skeleton guidance for PRM-based roadmap construction, expanding its utility to multi-query scenarios.

REFERENCES

- [1] J. Denny, R. Sandström, A. Bregger, and N. M. Amato, “Dynamic region-biased exploring random trees,” in *Alg. Found. Robot. XII*. Springer, 2020, (WAFR ‘16).
- [2] R. Sandstrom, D. Uwacu, J. Denny, and N. M. Amato, “Topology-guided roadmap construction with dynamic region sampling,” *IEEE Robotics and Automation Letters*, vol. 5, no. 4, pp. 6161–6168, 2020.

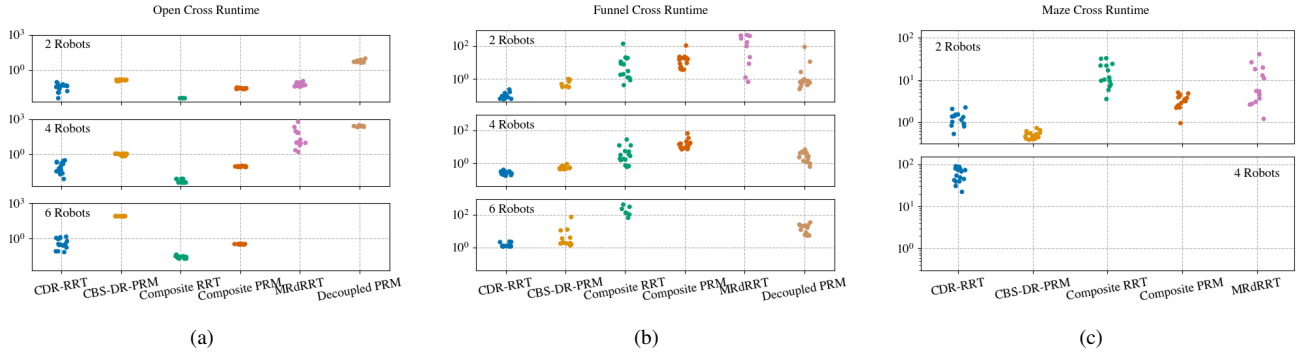


Fig. 10. Running time results for the Open Cross (a), Funnel Cross (b), and Maze Cross (b) environments for all methods. Those that were unable to find a solution within the time limit are omitted. We demonstrate improved scalability as compared to the other methods by consistently achieving low planning times even as the number of robots increases. On the larger (4 and 6-robot) scenarios with narrow passages, CDR-RRT achieves the lowest running time.

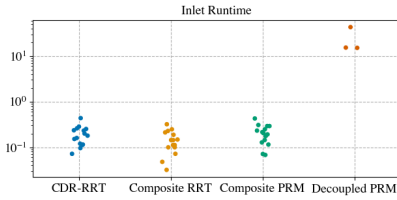


Fig. 11. Running time results for the Inlet environment. Although CDR-RRT, Composite RRT, and Composite PRM achieve similar average runtimes, CDR-RRT finds a lower cost solution.

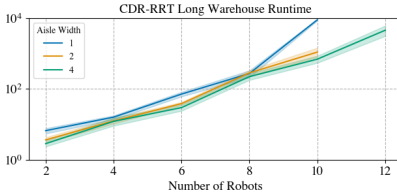


Fig. 12. Running time results for up to 12 robots for CDR-RRT on the Long Warehouse Environment.

[3] T. Lozano-Pérez and M. A. Wesley, “An algorithm for planning collision-free paths among polyhedral obstacles,” *Communications of the ACM*, vol. 22, no. 10, pp. 560–570, Oct. 1979.

[4] J. T. Schwartz and M. Sharir, “On the “piano movers” problem. ii. general techniques for computing topological properties of real algebraic manifolds,” *Advances in applied Mathematics*, vol. 4, no. 3, pp. 298–351, 1983.

[5] J. F. Canny, *The Complexity of Robot Motion Planning*. Cambridge, MA: MIT Press, 1988.

[6] L. E. Kavraki, P. Švestka, J. C. Latombe, and M. H. Overmars, “Probabilistic roadmaps for path planning in high-dimensional configuration spaces,” *IEEE Trans. Robot. Automat.*, vol. 12, no. 4, pp. 566–580, Aug. 1996.

[7] S. M. Lavalle, “Rapidly-exploring random trees: A new tool for path planning,” Iowa State University, Tech. Rep., 1998.

[8] D. Hsu, J.-C. Latombe, and H. Kurniawati, “On the probabilistic foundations of probabilistic roadmap planning,” *Int. J. Robot. Res.*, vol. 25, pp. 627–643, July 2006.

[9] S. Rodríguez, X. Tang, J.-M. Lien, and N. M. Amato, “An obstacle-based rapidly-exploring random tree,” in *Proc. IEEE Int. Conf. Robot. Autom. (ICRA)*, 2006.

[10] A. Yerzhova, L. Jaillet, T. Simeon, and S. M. Lavalle, “Dynamic-domain RRTs: Efficient exploration by controlling the sampling domain,” in *Proc. IEEE Int. Conf. Robot. Autom. (ICRA)*, Apr. 2005, pp. 3856–3861.

[11] I. Solis, J. Motes, R. Sandström, and N. M. Amato, “Representation-optimal multi-robot motion planning using conflict-based search,” *IEEE Robotics and Automation Letters*, vol. 6, no. 3, pp. 4608–4615, 2021.

[12] K. Solovey, O. Salzman, and D. Halperin, “Finding a needle in an exponential haystack: Discrete rrt for exploration of implicit roadmaps in multi-robot motion planning,” *The International Journal of Robotics Research*, vol. 35, no. 5, pp. 501–513, 2016.

[13] G. Sanchez and J.-C. Latombe, “Using a prm planner to compare centralized and decoupled planning for multi-robot systems,” in *Proc. IEEE Int. Conf. Robot. Autom. (ICRA)*, vol. 2, 2002, pp. 2112–2119.

[14] A. Dobson, K. Solovey, R. Shome, D. Halperin, and K. E. Bekris, “Scalable asymptotically-optimal multi-robot motion planning,” in *2017 international symposium on multi-robot and multi-agent systems (MRS)*. IEEE, 2017, pp. 120–127.

[15] R. Shome, K. Solovey, A. Dobson, D. Halperin, and K. E. Bekris, “drrt*: Scalable and informed asymptotically-optimal multi-robot motion planning,” *Autonomous Robots*, vol. 44, no. 3, pp. 443–467, 2020.

[16] L. Cohen, T. Uras, T. S. Kumar, and S. Koenig, “Optimal and bounded-suboptimal multi-agent motion planning,” in *Twelfth Annual Symposium on Combinatorial Search*, 2019.

[17] G. Wagner and H. Choset, “Subdimensional expansion for multirobot path planning,” *Artificial Intelligence*, vol. 219, pp. 1–24, 2015.

[18] M. Morales, L. Tapia, R. Pearce, S. Rodriguez, and N. M. Amato, “A machine learning approach for feature-sensitive motion planning,” in *Alg. Found. Robot. VI*. Springer, 2005, pp. 361–376, (WAFR ‘04).

[19] H. Kurniawati and D. Hsu, “Workspace importance sampling for probabilistic roadmap planning,” in *Proc. IEEE Int. Conf. Intel. Rob. Syst. (IROS)*, vol. 2, Sept. 2004, pp. 1618–1623.

[20] J. Berg and M. Overmars, “Using workspace information as a guide to non-uniform sampling in probabilistic roadmap planners,” in *Proc. IEEE Int. Conf. Robot. Autom. (ICRA)*, 2004, pp. 453–460.

[21] H. Kurniawati and D. Hsu, “Workspace-based connectivity oracle - an adaptive sampling strategy for prm planning,” in *Alg. Found. Robot. VII*. Springer, 2008, pp. 35–51, (WAFR ‘06).

[22] E. Plaku, L. Kavraki, and M. Vardi, “Motion planning with dynamics by a synergistic combination of layers of planning,” *IEEE Trans. Robot.*, vol. 26, no. 3, pp. 469–482, June 2010.

[23] J. Denny, R. Sandström, N. Julian, and N. M. Amato, “A region-based strategy for collaborative roadmap construction,” in *Alg. Found. Robot. XI*. Springer, 2015, pp. 125–141, (WAFR ‘14).

[24] H. Blum, “A transformation for extracting new descriptors of shape,” in *Models for Perception of Speech and Visual Form*, W. Wathen-Dunn, Ed. Cambridge, MA: MIT Press, 1967.

[25] A. Tagliasacchi, I. Alhashim, M. Olson, and H. Zhang, “Mean curvature skeletons,” *Computer Graphics Forum*, vol. 31, pp. 1735–1744, 08 2012.

[26] S. Bhattacharya, M. Likhachev, and V. Kumar, “Topological constraints in search-based robot path planning,” *Autonomous Robots*, vol. 33, no. 3, 2012.

[27] G. Sharon, R. Stern, A. Felner, and N. R. Sturtevant, “Conflict-based search for optimal multi-agent pathfinding,” *Artificial Intelligence*, vol. 219, pp. 40–66, 2015.